

Chemistry of photogenerated α -phenyl-substituted *o*-, *m*-, and *p*-quinone methides from phenol derivatives in aqueous solution

Li Diao and Peter Wan

Abstract: The enhanced photochemical reactivity of *o*-substituted phenols in its propensity to give *o*-quinone methide (*o*-QM) intermediates via excited state intramolecular proton transfer (ESIPT) was uncovered by Keith Yates as part of his now classic studies of photohydration of aromatic alkenes, alkynes, and related compounds. Photogeneration of QMs and the study of their chemistry along with potential biological applications are the focus of many groups. In this work, photochemical precursors to *o*-, *m*-, and *p*-QMs based on substituted phenols (hydroxybenzyl alcohols) and related compounds have been studied in aqueous solution as a function of pH and water content. The focus will be on QMs that are stabilized by an α -phenyl substituent, which enhances quantum yields for their formation, with the resulting QMs having longer lifetimes and easier to detect. Noteworthy is that all QM isomers can be photogenerated with the *o* and *m* isomers being the most efficient, consistent with the Zimmerman "ortho-meta" effect. *m*-QMs have formal non-Kekulé structures, and although they can be routinely photogenerated, are found to be most reactive. One *m*-QM was found to undergo a photocondensation reaction at high pH giving rise to *m*-substituted oligomers. The mechanism of QM formation in aqueous solution is believed to involve singlet excited phenols that undergo adiabatic deprotonation to give the corresponding photoexcited phenolate ion, which subsequently expels the hydroxide ion (photodehydroxylation). A pathway involving direct loss of water for the *o*-isomers is also possible in organic solvents.

Key words: quinone methides, phenols, excited state acidity, solvolysis, carbocations, meta effect, photopolymerization, non-Kekulé intermediates.

Résumé : La réactivité photochimique accrue des phénols *o*-substitués dans sa tendance à donner des intermédiaires *o*-quinométhides (*o*-QM) par le biais d'un transfert de proton intramoléculaire dans l'état excité (TPIIE) a été découverte par Keith Yates dans le cadre de ses études maintenant classiques sur la photohydratation des alcènes et des alcynes aromatiques et des composés apparentés. La photogénération de QM et l'étude de leur chimie en relation avec leurs applications biologiques potentielles sont les objets principaux de recherches de plusieurs groupes. Dans ce travail, opérant en solution aqueuse, on a examiné les précurseurs photochimiques de *o*-, *m*- et *p*-QM issus de phénols substitués (alcools hydroxybenzyliques) et de composés apparentés en fonction du pH et de la quantité d'eau présente. On s'est orienté vers les QM qui sont stabilisés par un substituant α -phényle, ce qui augmente les rendements quantiques de leurs formations et qui conduit à des QM de temps de vie plus longs et une plus grande facilité de détection. Il est important de noter que tous les isomères de QM peuvent être photogénérés, mais que les isomères *o*- et *m*- sont les plus efficaces; ce qui est en accord avec l'effet "ortho-méta" de Zimmerman. Les *m*-QM comportent des structures formelles qui ne correspondent pas à celles de Kekulé et qui, même si elles peuvent facilement être photogénérées, sont les plus réactives. On a trouvé qu'un QM subit une réaction de photocondensation à un pH élevé conduisant à la formation d'oligomères *m*-substitués. On croit que le mécanisme de formation des QM en solution aqueuse implique l'état singulet de phénols excités qui subissent une déprotonation adiabatique conduisant à la formation de l'ion phénolate excité correspondant qui expulse subséquemment l'ion hydroxyde (photodéshydroxylation). Une voie réactionnelle impliquant une perte directe d'eau à partir des isomères ortho est aussi possible dans les solvants organiques.

Mots-clés: quinométhides, phénols, acidité de l'état excité, solvolyses, carbocations, effet méta, photopolymérisation, intermédiaires qui ne correspondent pas à ceux de Kekulé.

[Traduit par la Rédaction]

Received 17 July 2007. Accepted 15 October 2007. Published on the NRC Research Press Web site at canjchem.nrc.ca on 9 November 2007.

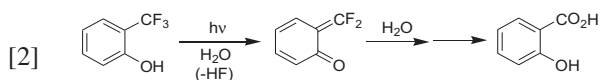
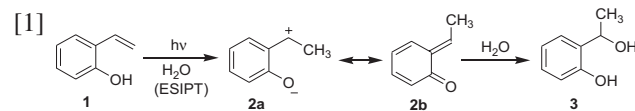
This article is dedicated to the memory of Professor Keith Yates.

L. Diao and P. Wan,¹ Department of Chemistry, Box 3065, University of Victoria, Victoria, BC V8W 3V6, Canada.

¹Corresponding author (e-mail: pwan@uvic.ca).

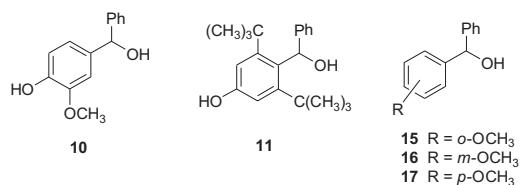
Introduction

The study of photochemical generation and structure-reactivity of polar intermediates derived from substituted aromatic compounds gained a new practitioner in Keith Yates, starting in the early 1980s. After a distinguished career studying classic organic reaction mechanisms (e.g., hydrolysis of esters and amides) and the behaviour of strong acids on organic compounds (acidity functions and their applications), Keith Yates decided to investigate how organic photochemistry could serve the study of organic reaction mechanisms, with initial work on the photohydration of aromatic alkenes and alkynes (1). The idea he had at the time was that the well-known phenomenon of enhanced acidity or basicity of many aromatic compounds (2) could manifest itself in enhanced reactivity such as hydrolysis or electrophilic attack, under the right conditions. Yates and co-workers successfully demonstrated the utility of their ideas in a series of papers that span over 15 years. In particular, in one their studies of photohydration Yates and Kalanderopoulos (3) proposed that the photohydration mechanism of *o*-hydroxystyrene (**1**) involved initial irreversible excited state intramolecular proton transfer (ESIPT) from phenol OH to the β -carbon of the alkene moiety, to give *o*-quinone methides (*o*-QM) **2a** and **2b**, which on trapping by water, would give the expected hydration product **3** (eq. [1]). This mechanism offers a reasonable explanation for the much lower photohydration efficiency observed for *o*-methoxystyrene. Yates and Kalanderopoulos (3) initially wrote only species **2a** as the proposed intermediate in the initial ESIPT step. However, one would expect that the dominant resonance contributor is **2b**, which has the well-known *o*-QM structure. Although Yates ultimately did not pursue a study of QMs, this initial paper (3) indicated that he was already at its doorstep. QM intermediates have a long history, but more recently it has become a topic of renewed interest in both thermal chemistry and photochemistry (4, 5). In particular, recent studies concerning biological applications of QMs as electrophiles for DNA cross-linking and general reactivity and (or) stability with deoxynucleosides as nucleophiles have appeared (5*j*–5*m*) that improve the current understanding along with demonstrated potential applications of these intermediates in biology. With respect to photochemical generation of QMs, initial systematic studies could be traced back to Seiler and Wirz (5*a*) who studied the photohydrolysis of a variety of trifluoromethylphenols and naphthols (e.g., eq. [2]) and demonstrated the viability of photogenerating a variety of difluoro-substituted QMs.



Continuing in the spirit of research direction laid out by Keith Yates, we reported a general method for photogenerating all of the parent QM isomers from

hydroxyl-substituted benzyl alcohols (5*c*, 5*d*). This method offered an efficient and general method for making a variety of simple QMs in aqueous solution — including all three parent systems — from simple phenol derivatives and takes direct advantage of the enhanced acidity of phenols in the excited singlet state. Moreover, hydroxybenzyl alcohols are readily available and have a high tendency to give polar intermediates in aqueous solution even though the hydroxide ion is considered to be a very poor leaving group. Although the method and proposed mechanism(s) of reaction are now well known amongst practitioners, many of the original details have not been published. It is the purpose of this paper to address this deficiency and to provide additional new reactivity data for compounds that have been studied before and also for new substrates. The results that will be reported are for hydroxybenzyl alcohols and related derivatives that have at least one α -phenyl substituent (**4**–**11** and **15**–**17**), the latter having the desirable effect of making these systems much easier to handle and study.



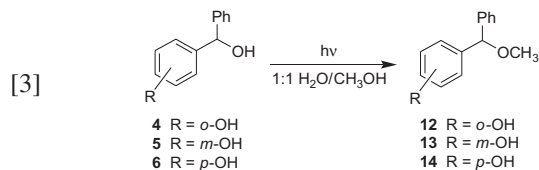
Results and discussion

Materials

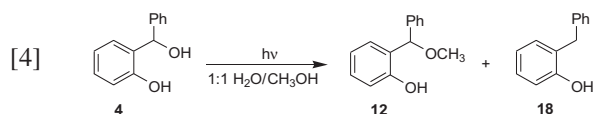
The compounds studied (**4**–**11** and **15**–**17**) were readily synthesized using standard procedures, most involving the use of Grignard reagents (see Experimental section).

Product studies

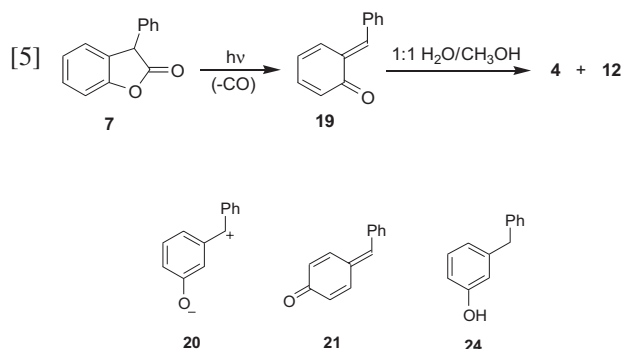
Photolysis of *o*-, *m*-, and *p*-hydroxybenzhydrols (**4**–**6**) in 1:1 (v/v) H_2O/CH_3OH (Rayonet photochemical reactor, 254 nm lamps, argon purged, 3 min) gave the corresponding methyl ethers **12** (17%), **13** (15%), and **14** (7%), respectively, as the only products in low conversion runs (<20%) (eq. [3]). The 1H NMR spectrum of the reaction mixture showed the characteristic methoxy singlet for the methyl ether product at δ 3.3–3.4. Similar photolysis of their methoxy-substituted analogs (**15**, **16**, and **17**) gave no reaction except for **15**, which gave about 4% of the corresponding methyl ether. Control experiments performed in the absence of light indicated that only the *o* and *p* isomers were reactive (yield up to 5%) if a small amount of $NaHCO_3$ was not added to the solution prior to photolysis. Therefore, all runs (photochemical and thermal) using CH_3OH were carried out in the presence of a pinch of $NaHCO_3$. It is postulated that the residual thermal reaction (solvolysis) in the absence of added $NaHCO_3$ is due to traces of acid present in CH_3OH .



Prolonged photolysis (>20 min) of **4–6** gave increasing yields of the methyl ether and also formation of a secondary benzylphenol product (e.g., eq. [4]), which has a characteristic singlet at δ 4.0. As shown in Fig. 1 for **4**, the yield of methyl ether **12** rises rapidly within the first 20 min of irradiation after which its formation slows down and levels off at about 60% yield, while benzylphenol **18** builds up in the product mixture although never becoming a major product. It is reasonable to propose that **18** is the secondary product from photolysis of **12**. The mechanism probably involves initial homolytic cleavage of the C–OMe bond, followed by a disproportionation of the radical pair to form **18** and formaldehyde. We have shown (6) that related benzyl methyl ethers react this way on photolysis.



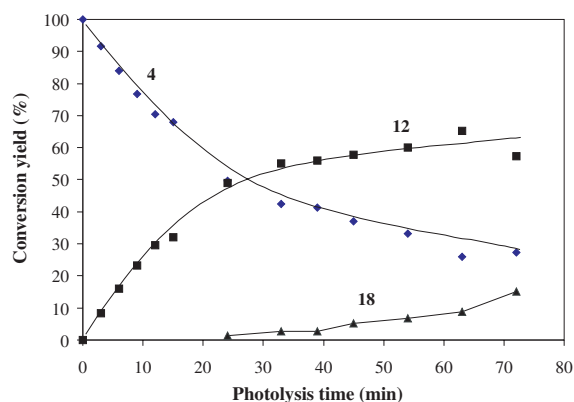
Irradiation of coumaranone **7**, a known photoprotonator (7) of *o*-QM **19**, gave **12** as the only product (~3% yield) under identical conditions as used for **4**. Extended photolysis (254 nm, 8 min), however, resulted in both methyl ether **12** (~13%) and benzhydrol **4** (~9%) as products (eq. [5]). These results are consistent with a mechanism of reaction via *o*-QM **19** from the photolysis of **7** via a standard photodecarbonylation mechanism. Since the photolysis of **4** resulted in similar chemistry, it is reasonable to suggest that *o*-QM **19** is also the essential intermediate in the photolysis of **4**. Following this rationale, the photomethanolysis of **5** and **6** are proposed to proceed via *m*- and *p*-QMs **20** and **21**, respectively. These proposals are confirmed in UV–vis and laser flash photolysis (LFP) studies (vide infra).



Photolysis of α,α -diphenyl-substituted systems **8** and **9** in 1:1 $\text{H}_2\text{O}/\text{CH}_3\text{OH}$ under identical conditions as for **4** and **5** resulted in significantly higher conversions to the corresponding methyl ethers (28% and 60%, respectively). Secondary photochemistry to give the reduced disproportionation products (vide supra) were not observed under the conditions employed. One possible reason for the lack of secondary photochemistry for these compounds is that the increased steric hindrance at the benzylic position (two phenyl groups) retards biradical disproportionation.

The effect of solution pH (aqueous portion) was examined. Acidic pH (pH < 4) could not be employed in product studies for the *o* and *p* isomers because of significant residual thermal reaction. Therefore, only the pH 7–14 range was

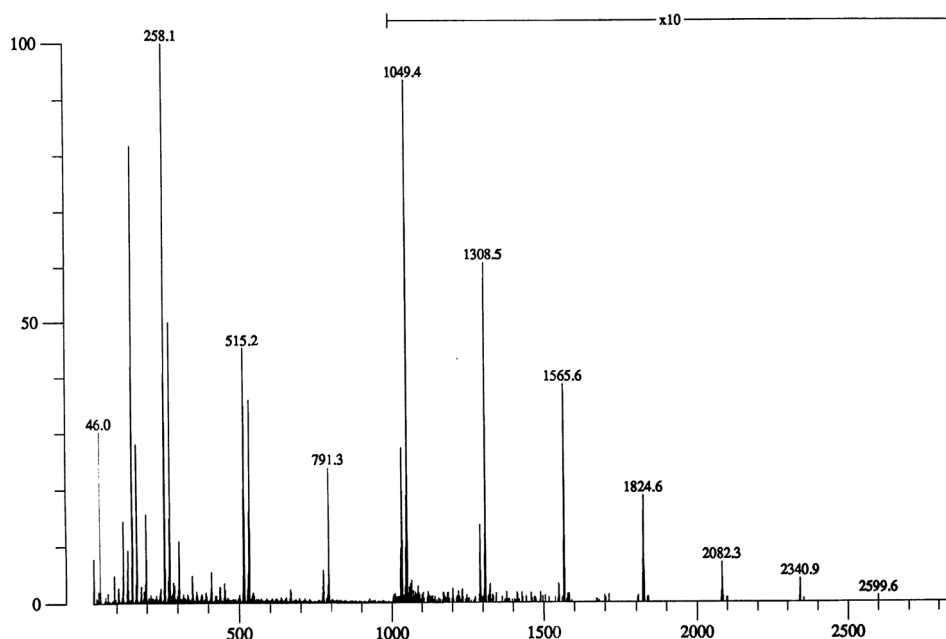
Fig. 1. Plot of the photochemical conversion of **4** to **12** and **18** in 1:1 $\text{H}_2\text{O}/\text{MeOH}$ as a function of photolysis time (λ_{ex} 254 nm).



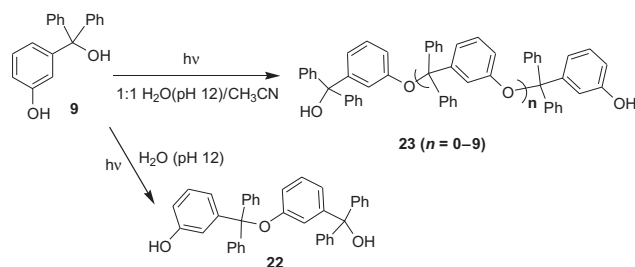
examined for all substrates, although acidic pH levels were used for selected *m* isomers. In all cases, higher conversions to the methyl ethers were observed at higher pH values. For example, a plot of yield of **12** vs. pH (from 7–14) from photolysis of **4** in 1:1 $\text{H}_2\text{O}/\text{CH}_3\text{OH}$ showed a sigmoid curve in the pH 11–13 range with an apparent inflection point at around 12. Since phenols have $\text{p}K_{\text{a}}(\text{S}_0)$ in the 9–12 range (in neat water), the increase in reaction efficiency at high pH is consistent with higher reactivity observed on directly exciting the phenolate ion. Indeed, the apparent $\text{p}K_{\text{a}}$ of **4** in 1:1 $\text{H}_2\text{O}/\text{CH}_3\text{OH}$, as determined by UV–vis spectrometry, was estimated to be about 12.

Photolysis of *m* isomers **5** and **9** in basic solution resulted in the formation of a cloudy solution. It was more pronounced for the α,α -diphenyl derivative **9** and not observed for all *o* and *p* isomers. Initial MS analysis of the precipitate showed formation of dimers and trimers, suggesting that a photoinitiated self-condensation pathway may be operative for the *m* isomers. To enhance the yield of these condensation products, photolysis of **9** was carried out in neat water at pH 12 to avoid the presence of CH_3OH acting as a nucleophile. Photolysis (10 min) gave a cloudy solution that was subsequently neutralized and extracted with CH_2Cl_2 . The ^1H NMR spectrum of the product mixture showed a group of new peaks including two exchangeable protons (hydroxy singlets at δ 5.1 and 8.2) and a triplet near the aromatic region (δ 6.4), in addition to those expected for **9**. Prolonged irradiation (30 min) caused the formation of pale yellow flakes that precipitated out of solution and aggregated upon the addition of salt. This yellow substance gave a much cleaner ^1H NMR spectrum in which there are twice as many aromatic protons as hydroxyl protons than in the starting material and a $\text{M}^+ - 1$ of 533 (negative FAB), indicative of a dimeric structure. There are two pathways in which a dimer can arise. A “head-to-tail” dimerization pathway to give dimer **22** or electrophilic aromatic substitution of the diphenylmethyl moiety (as the cation) onto the phenolate (more activated) ring, which would give a tetraphenylmethane-type structure. We believe a head-to-tail pathway has occurred to give **22** (Scheme 1), since treatment of this dimer (and longer oligomers, vide infra) in mild acid (pH 1) in 1:1 $\text{H}_2\text{O}/(\text{CH}_3)_2\text{CO}$ gave back starting material **9**. Such a reversible reaction in mild acid would be anticipated for a highly activated benzylic ether linkage but not for the alter-

Fig. 2. Mass spectrum (negative ion FAB) of photoproduct **23** obtained on photolysis of **9** in 1:1 H₂O (pH 12)/CH₃CN. The highest mass observed at 2856 ($n = 9$; see Scheme 1) is not shown. All others from $n = 8$ to $n = 0$ match the expected masses reasonably well.



Scheme 1.



native tetraphenylmethane structure. Interestingly, similar photolysis of **9** in basic 1:1 H₂O/CH₃CN gave a yellow homogeneous solution after 30 min photolysis, which upon work-up was found to contain oligomers **23** of up to 11 units by negative ion FAB MS (Scheme 1, Fig. 2). The chemistry observed here for *m* isomer **9** is consistent with an *m*-QM intermediate that has a zwitterionic structure (**20** from **5** or **32** from **9**). In basic pH, the starting material **9** is in the (nucleophilic) phenolate form and shows great propensity to attack the positive charge of the *m*-QM structure, hence dimerization and oligomerization. Moreover, *m*-QM from **9** is longer lived than the corresponding QM from **5** (vide infra) and hence more prone to attack by the phenolate ion. The *o*- and *p*-QMs **19** and **21** are less reactive (they have a neutral quinoid structure) in this respect and dimerization and oligomerization is not as prominent, although it has also been reported for an *o* isomer under extended photolysis (**8**) and also in the photolysis of (2-hydroxybenzyl)trimethylammonium iodide precursor (**5j**), both in basic solution.

Quantum yields

Quantum yields for methyl ether formation for selected substrates were measured in 1:1 H₂O/CH₃OH using the

Table 1. Quantum yields (Φ_p) for methyl ether formation

Compound	Φ_p
4	0.46 ± 0.03
15	0.11
7	0.08
8	0.76
5	0.23
6	0.19
17	0.0

Note: In 1:1 (v/v) H₂O/CH₃OH. Measured using **4** as the secondary actinometer. Photolyses were carried out in a Rayonet RPR reactor (λ_{ex} 254 nm). Estimated errors are 10%–15% of quoted value. Conversions were kept <30%.

photomethanolysis of **4** ($\Phi_p = 0.46$) (**5c**) as a secondary actinometer (λ_{ex} 254 nm). Although in general, product quantum yields cannot be used as a direct measure of reactivity, comparisons of Φ_p values in Table 1 reveal that the hydroxyl-substituted alcohols have much higher quantum yields than their methoxy-substituted counterparts. The addition of an extra α -phenyl group also enhances quantum yield. Furthermore, *o* and *m* isomers have higher quantum yields than *p* isomers, which is consistent with Zimmerman's "ortho–meta" effect (**9**) for photoreactivity of substituted benzenes that undergo reaction via polar intermediates.

UV–vis studies

Selected *o* and *p* substituted isomers were studied using UV–vis spectrophotometry in aqueous CH₃CN (to avoid complications from methyl ether formation if MeOH was used) to gain insight into whether the corresponding pro-

Fig. 3. Absorption spectra of **4** in pure CH₃CN. (a) (full line) before photolysis, (b) immediately after 4 min photolysis (8 × 254 nm lamps) at -15 °C, (c) on standing for 3 h at RT, (d) (dashed line) standing overnight at RT.

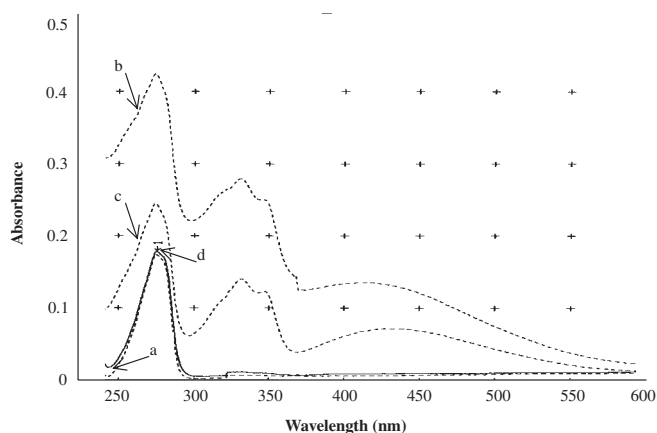


Table 2. Solvent effect on absorption maxima (λ_{max}) for *o*-QM **19** photogenerated from **4**.

Temperature (°C)	Solvent	λ_{max} (nm)	λ_{max} (nm)
<0 ^a	cyclohexane	333	410
	THF	333	427
	CH ₃ CN	332	434
ca. 5	1:9 H ₂ O/CH ₃ CN	333	438
ca. 20	1:1 H ₂ O/CH ₃ CN ^b	345	455

^aIrradiated (254 nm) in an ethylene glycol/dry ice slurry (ca. -15 °C).

^bResults from LFP studies.

posed QMs are observable without the need for LFP. None of the *m* isomers gave observable transients using standard UV-vis techniques and *m*-QM intermediates could only be observed using LFP (vide infra).

Photolysis of **4** in neat CH₃CN (~10⁻² mol/L, 254 nm for ~1–5 min) in a quartz cuvette resulted in the formation of a initially yellow, then orange-red, and eventually a deep red-brown solution. UV-vis spectra were recorded before and after photolysis and are shown in Fig. 3 where the starting material absorbs only below 300 nm, with λ_{max} at 276 nm. On photolysis, the appearance of new absorption bands at 333 and 423 nm indicated the formation of a new species. This transient decayed slowly in neat CH₃CN; the yellow color remained even on sitting overnight. A similar transient was observed in THF and cyclohexane (at ca. -15 °C) (Table 2). The red shift of λ_{max} on going to more polar solvents indicate that these transitions of π, π^* in character, consistent with a highly conjugated *o*-QM **19**.

Photolysis of **4** in 1:9 H₂O/CH₃CN at ~5 °C produced an orange-red solution, which was formed more efficiently than in neat CH₃CN but with similar λ_{max} (Table 2). Upon removal from the UV source, the color gradually faded ($\tau \approx 40$ s; shorter at 20 °C) with complete recovery of the UV spectrum prior to irradiation. When photolyzed in essentially neat H₂O (<5% CH₃CN as co-solvent), the same orange-red transient was generated but disappeared quickly ($\tau < 5$ s), preventing the recording of a UV-vis spectrum.

Table 3. Absorption maxima (λ_{max}) and estimated lifetimes (τ) of photogenerated transient QMs from hydroxybenzhydrols.

Compound	Solvent ^a	λ_{max} (nm) ^b	τ ^c
4	100% H ₂ O	333, 438	<5 s
	1:9 H ₂ O/CH ₃ CN	333, 438	27 s
	1:9 H ₂ O/CH ₃ CN (~5 °C)	333, 438	40 s
6	H ₂ O	372	10 s
	1:1 H ₂ O/CH ₃ CN	360	216 s
10	1:9 H ₂ O/CH ₃ CN	354	>60 min
	pH 7 buffer	377	130 s
11	1:1 H ₂ O/CH ₃ CN	377	>60 min
	pH 7 buffer	356	>60 min
11	1:1 H ₂ O/CH ₃ CN	356	>60 min

^aAt ~20 °C unless otherwise specified.

^bError is ca. 2 nm.

^cEstimated lifetime from a fit to a single exponential decay.

Similar photolysis of *p*-hydroxybenzhydrols **6**, **10**, and **11** in aqueous CH₃CN also gave red colored transients, but none was capable of giving such a colored transient when photolyzed in neat CH₃CN. The transient from **6** absorbed strongly at 372 nm in H₂O (<5% CH₃CN) with a 10 s lifetime. It was 20 times longer-lived in 1:1 H₂O/CH₃CN ($\tau = 216$ s.). Similar transient absorptions were observed for **10** (at 377 nm) and for **11** (at 356 nm) in either neat water or in 1:1 H₂O/CH₃CN. Table 3 summarizes the λ_{max} and τ for the transients observed. All of the observed transients return to starting materials eventually. The transient from **6** (*p*-QM **21**) has a longer lifetime than that from **4** (*o*-QM **19**). Electron-donating groups on the benzene ring (in **10** and **11**) produce transients that are even longer-lived and hence may be thought of as stabilizing substituents. This result is consistent with recent results of Rokita and co-workers (5*m*) in their study of *o*-QM adducts of deoxynucleotides. All of these observations are consistent with the transients being assignable to the corresponding *p*-QMs.

Fluorescence measurements

There is now considerable evidence supporting singlet state reactivity for substituted benzenes (without carbonyl substituents) undergoing photochemical reactions that gives rise to ionic (polar) intermediates (1–3, 5, 6). Earlier studies (5*c*, 5*d*, 6*c*) have shown that it is the singlet excited state of the precursor phenols that give rise to QMs. Nevertheless, fluorescence studies can give much additional ancillary data regarding mechanism and reactivity that cannot be easily obtained by other means.

o-Hydroxybenzyl alcohols **4** and **8** gave similar fluorescence emissions centered at ~300 nm in neat CH₃CN. The fluorescence quantum yields (Φ_f) measured using anisole ($\Phi_f = 0.29$ in cyclohexane) as secondary standard (10) were drastically reduced by H₂O addition, accompanied by the red-shifted emission maxima (Table 4). Of the two alcohols, the fluorescence intensity of **4** was affected the most, where only a weak emission band was observed beside a clearly visible Raman band in 100% H₂O. The fluorescence lifetimes (τ) were essentially the same in 100% CH₃CN but were drastically decreased with increased water concentration. Similar fluorescence emissions were observed for two related derivatives of **4** (**15**, **18**) in the above mentioned sol-

Table 4. Effect of H₂O content in CH₃CN on emission maximum (λ_{max}), fluorescence quantum yields (Φ_{f} , excited at 270 nm), and lifetimes (τ , excited at 275 nm) of *ortho*-substituted compounds.

	Solvent	4	8	15	18
λ_{max}	100% CH ₃ CN	298	299	299	297
	1:1 CH ₃ CN/H ₂ O	302	304	—	299
	100% H ₂ O	—	—	300	—
Φ_{f}^a	100% CH ₃ CN	1 (0.13)	1 (0.092)	1 (0.28)	1 (0.25)
	1:1 CH ₃ CN/H ₂ O	0.21	0.48	—	0.47
	100% H ₂ O	0.04	0.12	0.62	0.10
τ^b (ns)	100% CH ₃ CN	4.5	4.6	5.3	5.1
	1:1 CH ₃ CN/H ₂ O	1.3	<2	4.6	3.0
	100% H ₂ O	—	—	1.9	<1

^aMeasured using anisole ($\Phi_{\text{f}} = 0.29$ in cyclohexane) as secondary standard (10). Absolute quantum yield quoted in brackets. All other numbers are relative yields.

^bMeasured using PTI LS-1 time-correlated single photon counting system.

Table 5. Effect of H₂O content (in CH₃CN) on emission maximum (λ_{max}), fluorescence quantum yields (Φ_{f} , excited at 270 nm), and lifetimes (τ , excited at 275 nm) of *meta*-substituted compounds.

	Solvent	5	16	24	9
λ_{max}	CH ₃ CN	296	295	293	299
	1:1 H ₂ O/CH ₃ CN	299	295	297	302
	H ₂ O	—	296	297	—
Φ_{f}^a	CH ₃ CN	1 (0.22)	1 (0.21)	1 (0.25)	1 (0.21)
	1:1 H ₂ O/CH ₃ CN	0.38	0.95	0.79	0.46
	H ₂ O	0.08	0.67	0.24	0.13
τ^b (ns)	CH ₃ CN	5.4	—	5.0	4.9
	1:1 H ₂ O/CH ₃ CN	1.9	—	4.5	—
	H ₂ O	<1	—	1.3	<1

^aMeasured using anisole ($\Phi_{\text{f}} = 0.29$ in cyclohexane) as secondary standard (10). Absolute quantum yield quoted in brackets. All other numbers are relative yields.

^bMeasured using PTI LS-1 time-correlated single photon counting system.

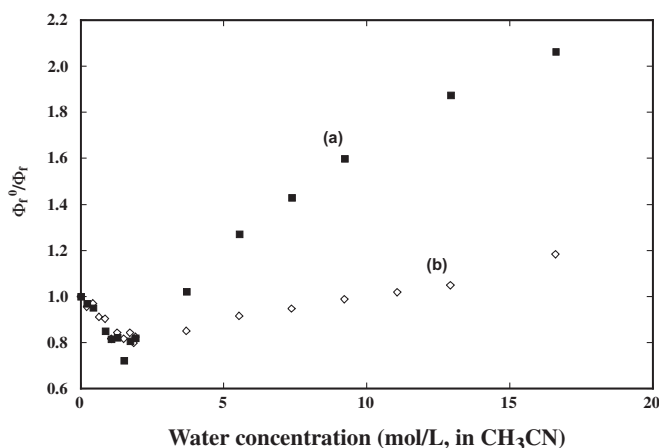
vent systems. Measurement of Φ_{f} revealed that the fluorescence of **18** was quenched by 90% in 100% H₂O, while the fluorescence of **15** was much less sensitive to the presence of water than that of **4** and **18**. The fluorescence lifetimes (τ) of **18** has an initial decrease to 3 ns in 1:1 H₂O/CH₃CN and then to <2 ns in 100% H₂O, while the τ of **15** was almost unchanged by the addition of 50% water and then dropped to 1.9 ns in 100% H₂O. Thus, the overall magnitude of water effect on these three compounds followed the order **4** > **18** > **15**. The lack of a fluorescence quenching effect for **15** can be attributed to its lack of a phenol moiety. Similar trends in fluorescence behaviour were observed for a series of *m*-substituted compounds (Table 5).

Fluorescence emissions of **4** and **8** were also observed in aqueous solutions of different pH values. However, their fluorescence emissions were in general so weak that it was not feasible to accurately measure the fluorescence quantum yield. Therefore, relative fluorescence intensity measurements ($\Phi_{\text{f}}^{\text{o}}/\Phi_{\text{f}}^{\text{pH 7}}$; $\Phi_{\text{f}}^{\text{o}}$ = fluorescence quantum yield at pH 7) at ~290 nm were employed. No emission was observed in basic solution (0.1 N NaOH) for either *ortho* compound. Since their UV-vis spectra showed growth of the absorption of the

corresponding phenolate ion (~290 nm) in basic media, excitation at 290 nm gave weak emissions at ~350 nm, which presumably are the fluorescence emissions of the corresponding phenolate. Similar experiments with phenol itself gave a weak emission at 335 nm, while *o*-cresol gave a weak emission at 346 nm. These weak signals indicate that excited phenolate ions are photochemically reactive, i.e., they decay through other routes competitive with fluorescence emission.

Stern-Volmer type plots of fluorescence quenching by added water (in CH₃CN solution) were carried out for a number of substrates. All the phenols displayed increasing fluorescence emission on the addition of small amounts of water (up to about 2 mol/L water) after which the fluorescence was quenched. The addition of initial water results in hydrogen bonding to the phenol OH (and to benzylic alcohol OH) resulting in a water-substrate complex that is more fluorescent than the substrate alone in CH₃CN. Addition of more water causes quenching of fluorescence due to water-mediated proton transfer from phenol OH to solvent. For those alcohols that can give rise to QMs, the addition of water also promotes the photodehydroxylation pathway. Indeed,

Fig. 4. Stern–Volmer plot of relative fluorescence intensity (Φ_f^0/Φ_f) vs. water concentration in CH_3CN for **4** (λ_{ex} 270 nm).



these substrates (e.g., **4–6**) are quenched more efficiently by water. A particularly informative Stern–Volmer type plot is shown in Fig. 4 in which H_2O and D_2O were employed as quenchers (in CH_3CN) for **4**. There was no observable solvent isotope effect in the enhanced fluorescence observed at low water content. However at higher water content, H_2O quenched significantly more efficiently (up to twofold) than D_2O at the same concentration. This is consistent with a mechanism of reaction in which **4** undergoes a concerted loss of H_2O (D_2O) assisted by solvent water to form *o*-QM **19**. A mechanism involving initial simple phenol ionization to solvent water such as that only available in **18** would not give rise to such a large solvent isotope effect.

Nanosecond laser flash photolysis (LFP)

The UV–vis studies described earlier have already shown that *o*- and *p*-QMs are observable under certain conditions. However, *m*-QMs are presumably too short-lived for this technique. Use of LFP should provide a better picture for whether transients can be assigned to all QM isomers and their relative efficiency for formation under various conditions and hence provide additional insights into reaction mechanism.

LFP of **4** in 1:1 $\text{H}_2\text{O}/\text{CH}_3\text{CN}$ under either N_2 or O_2 gave the same strong signals as reported in the already mentioned UV–vis studies, with no observable decay within the millisecond range, the limit of the nanosecond LFP system. A significant amount of transient was also formed on photolysis in neat CH_3CN (under either N_2 or O_2), although the absorption bands were significantly blue-shifted (the 455 and 345 nm bands were shifted to 410 and 330 nm, respectively). Relative quantum yields for the formation of the transients as a function of water content in CH_3CN were measured by monitoring the ΔA at both 350 and 450 nm (Fig. 5). Interestingly, the yield of the transient decreased initially (at low water content), followed by a dramatic increase with the increase in water concentration. This observation corroborates the enhanced fluorescence emission observed at low water content and suggests that when the substrates is hydrogen-bonded to small amounts of water, it is *less* reactive than without water. When the water content reaches above 2 mol/L the compound becomes more reac-

Fig. 5. Relative quantum yields for the formation of *o*-QM **19** from **4** as a function of water content (in CH_3CN) as monitored at 350 and 450 nm using LFP (λ_{ex} 266 nm).

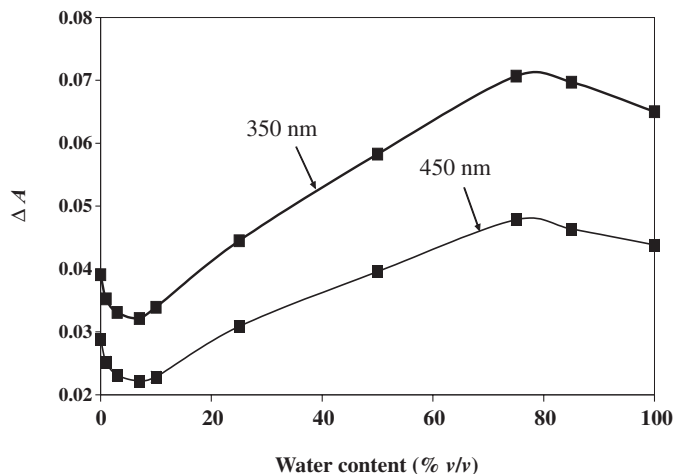
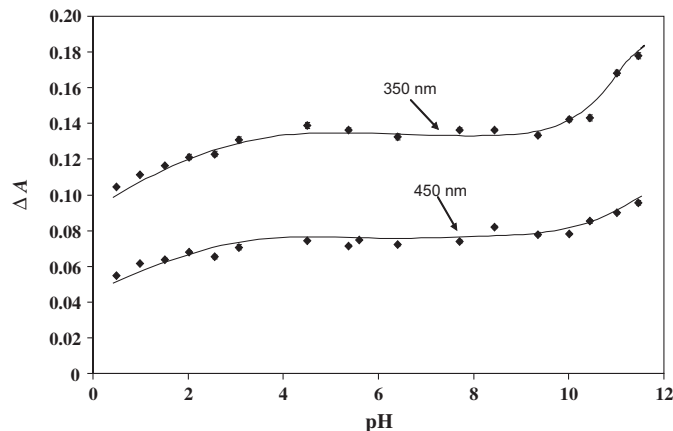


Fig. 6. Relative quantum yields (ΔA) for the formation of *o*-QM **19** from **4** vs. pH, monitored at 350 and 450 nm using LFP in neat H_2O (λ_{ex} 266 nm).



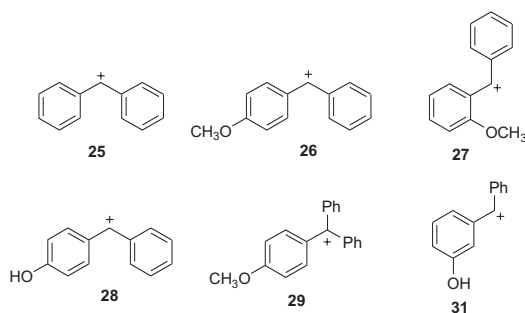
tive, consistent with a water-mediated mechanism. The maximum yield was reached in ca. 75% $\text{H}_2\text{O}/\text{CH}_3\text{CN}$, which was followed by a slight drop on approaching 100% H_2O .

Transient spectra from **4** were also taken in neat H_2O at different pH values with the same transient being observed in the whole pH range. A plot of ΔA (relative quantum yield) vs. pH (Fig. 6) showed two “titration” regions, at pH ~1 to 2, and at pH 11 to 12. The first of these is shallow and not prominent but approximately corresponds to the $\text{p}K_{\text{a}}(\text{S}_1)$ of phenols, whereas the second corresponds to $\text{p}K_{\text{a}}(\text{S}_0)$. Although we were not able measure yields for methanolysis in acid for **4** because of competing thermal reactions, the LFP method is not encumbered by this problem since it monitors for transient QM formation on excitation. The “shallow” titration curve at low pH suggests that excited state proton dissociation prior to reaction is important but that there may also be an independent acid-catalyzed pathway operating at these values of pH that involves an acid-mediated loss of water followed by deprotonation of the phenol OH to give the QM. The lifetimes of this transient (pseudo first-order

decays) were measured between pH 0 and 5 (above pH 5 the lifetimes were too long for the detection system employed). A plot of $\log k_{\text{obs}}$ vs. pH gave a slope of -1 indicating that the transient has an acid-catalyzed pathway for reaction (with $k_{\text{H}^+} = 1.0 \times 10^6 \text{ (mol/L)}^{-1} \text{ s}^{-1}$), in general agreement with results of Kresge and co-workers (5f–5h) and McClelland et al. (5i).

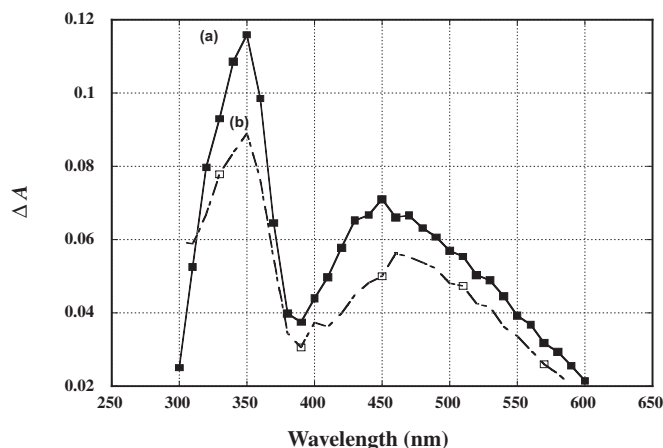
LFP of **7** in 1:1 $\text{H}_2\text{O}/\text{CH}_3\text{CN}$ afforded a transient spectrum essentially identical to that observed for **4** but with much weaker signal intensity, consistent with the lower reactivity of photomethanolysis and photohydration observed for **7**. Since **7** is known to give *o*-QM **19** upon photolysis (7), it is reasonable to infer that the transient from **4** is indeed *o*-QM **19**.

LFP of the *o*-methoxy derivative **15** in 1:1 $\text{H}_2\text{O}/\text{CH}_3\text{CN}$ gave a weak absorption at 420 nm, with a short-lived (13 ns) and a longer-lived species ($\sim 0.5 \mu\text{s}$) (fitted to the sum of two single exponential decays). These transients are very different from those observed for **4**. Chateaneuf (11) found that the diphenylmethyl cation (**25**) has λ_{max} at 435 nm with ~ 1 ns lifetime by using picosecond LFP, while McClelland and co-workers (12) reported that (*p*-methoxyphenyl)phenyl methyl cation (**26**) absorbs at 455 nm with a $0.5 \mu\text{s}$ lifetime in 2:1 $\text{H}_2\text{O}/\text{CH}_3\text{CN}$. Since the LFP system used by the McClelland group has a pulse of ~ 20 ns, they were unable to observe the short-lived species. Considering that substituents on the benzene ring have similar electron donating and withdrawing abilities at the ortho and para positions, it is reasonable to propose that the ortho-substituted diphenylmethyl cations also absorb in the 400–500 nm region and have microsecond lifetimes. Therefore, the long-lived ($\sim 0.5 \mu\text{s}$) species observed from **15** is assigned to carbocation **27**. Since Peters and Li (13) showed that the contact ion pair from diphenyl chloride had a lifetime of 150 ps, the short-lived (13 ns) species that we observed may be a radical cation.

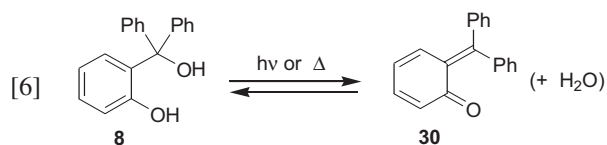


LFP of *p*-hydroxybenzhydrol (**6**) gave one strong absorption band at 360 nm with no observable decay within ms range in 1:1 $\text{H}_2\text{O}/\text{CH}_3\text{CN}$, under either N_2 or O_2 . The signal was also observed in 5% $\text{H}_2\text{O}/\text{CH}_3\text{CN}$ but not in neat CH_3CN . The yield of the transient (as measured by ΔA) increased with the increase in the water content to a maximum at 75% $\text{H}_2\text{O}/\text{CH}_3\text{CN}$. The transient absorption spectrum observed for the *p*-methoxy analog **17** had a weak band at 455 nm with small shoulders at 340 and 360 nm. Monitored at 455 nm, the decay consisted of two components, one with ~ 45 ns lifetime and another with a $\sim 1 \mu\text{s}$ lifetime. The lifetime of the longer-lived species decreased significantly with increasing water content. In 0.5 mol/L NaOH, essentially no signal was observable in 400–500 nm region. These facts

Fig. 7. Transient absorption spectra observed from **8** by LFP under O_2 in (a) pH 7 and (b) pH 12 in 1:1 $\text{H}_2\text{O}/\text{CH}_3\text{CN}$ ($\lambda_{\text{ex}} 266 \text{ nm}$).



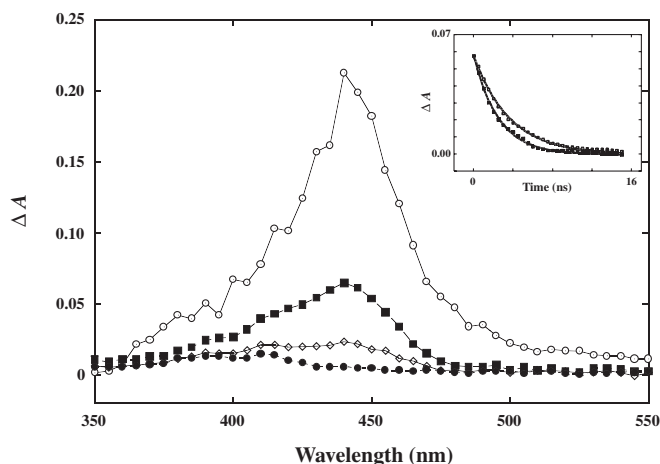
imply that the transient has cationic character. According to McClelland and co-workers (12) (*p*-methoxyphenyl)phenyl methyl cation (**26**) has $\lambda_{\text{max}} = 455 \text{ nm}$ in CH_3CN (diarylmethyl chloride as precursor), which is also accompanied by the (*p*-methoxyphenyl)phenylmethyl radical at 340 nm. The cation has a lifetime of $0.5 \mu\text{s}$ in 2:1 $\text{H}_2\text{O}/\text{CH}_3\text{CN}$. The long-lived species generated from **17** has absorption characteristics and lifetime that matches those of **26**. Although the transient generated from **6** ($\tau = 216 \text{ s}$ in 1:1 $\text{H}_2\text{O}/\text{CH}_3\text{CN}$, vide supra) has similar absorption characteristics as cation **26**, it is too long-lived to be **28**. It seems reasonable that the transient is that of *p*-QM **21** consistent with it being much less reactive. Similarly, the transients observed for **10** and **11** (vide supra), which were quenchable by water and had even longer lifetimes than *p*-QM **21** are also the respective *p*-QMs.



LFP of triphenyl alcohol **8** produced a strongly absorbing transient in either neat acetonitrile or in 1:1 $\text{H}_2\text{O}/\text{CH}_3\text{CN}$ (Fig. 7), with no observable decay within 2 ms. The transient spectrum is almost identical to those obtained from **4** and **7**, indicating that a similar transient was being generated by all of these compounds and the additional phenyl substitution on benzylic carbon had little effect on absorption characteristics. McClelland et al. (12b) have reported that the (*p*-methoxyphenyl)diphenylmethyl cation **29** has a lifetime of 0.71 ms in 2:1 $\text{H}_2\text{O}/\text{CH}_3\text{CN}$, which is much shorter than the transient observed from **8**. Using the same rationale as for the benzhydrols, the transient observed for **8** is most likely *o*-QM **30**. Moreover, it is known that **8** and related compounds are thermo and photochromic and their coloured forms are believed to be due to their corresponding *o*-QM structures, with absorptions bands at 340 and 440 nm (14) (eq. [6]).

LFP of **5** in 1:1 $\text{H}_2\text{O}/\text{CH}_3\text{CN}$ (O_2 purged) generated a strongly absorbing but short-lived transient with $\lambda_{\text{max}} = 440 \text{ nm}$ and a 30.1 ns lifetime (Fig. 8). This species was in-

Fig. 8. Transient absorption spectra observed for **5** (assigned to **20**) in 1:1 H₂O/CH₃CN (O₂) (λ_{ex} 266 nm). Top to bottom: recorded 10, 40, 80, and 200 ns after the laser pulse (Inset: top without ethanolamine and bottom with 0.24 mol/L ethanolamine, monitored at 450 nm).



sensitive to oxygen and quenchable by water, added NaBH₄, and ethanolamine. A weak residual signal (390 and 410 nm) was observable after the 440 nm transient had decayed (Fig. 8, bottom trace), which is more predominant with decreased water content. LFP of **5** in neat CH₃CN under N₂ gave two strong signals at 330 and 410 nm, respectively, both of which disappeared with O₂ purging. No 440 nm transient was observed. LFP of *m*-methoxybenzhydrol (**16**) generated a short-lived transient with a lifetime of 75.5 ns and a long-lived one of 6.3 μs ($\lambda_{\text{max}} = 428$ nm) in 1:1 H₂O/CH₃CN (O₂). A similar LFP study of *m*-benzylphenol (**24**) gave a weak but long-lived transient at around 400 nm and a short-lived one at 750 nm. Both long-lived species from **16** and **24** might be the radical cation formed from an electron ejection, which is not the same as either transient from **5**. The relative quantum yield of formation of the 440 nm (ΔA_{440}) transient increased with increasing pH (in 1:1 H₂O/CH₃CN, lifetimes and ΔA_{440} could not be accurately measured at all pH values in 100% water because of acid quenching). The resulting plot of ΔA_{440} vs. pH showed a titration curve in basic pH at an apparent $\text{p}K_{\text{a}}(\text{S}_0)$ value of 12 and a $\text{p}K_{\text{a}}(\text{S}_1)$ of 2. A plot $\log k_{\text{obs}}$ vs. pH in 1:1 H₂O/CH₃CN showed that the lifetimes were unchanged between pH 4 and 11 and were shortened in either acidic or basic media.

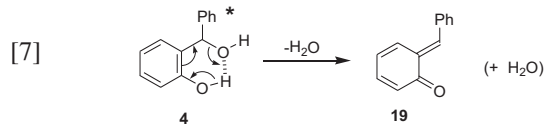
The λ_{max} and band shape of the 440 nm transient observed on LFP of **5** is essentially identical to that of the corresponding diarylmethyl cations reported by McClelland et al. (12*b*). Although they did not photogenerate the exact *m*-hydroxy-substituted cations, the lifetimes of those that were reported are informative. For example, diarylmethyl cations without strongly electron donating substituents have lifetimes of less than 10 ns in aqueous solution and are not detectable by standard nanosecond LFP; τ was estimated to be 1 and 5 ns for the **25** and the (*p*-methylphenyl)phenylmethyl cations, respectively. Clearly, the transient observed from **5** is similar to an arylmethyl carbocation, but its lifetime is too long to be simply the (*m*-hydroxyphenyl)phenylmethyl cation (**31**). Additional evidence available is that the methoxy derivative

of **16** did not produce any cationic transient by LFP. Moreover, **5** gave a significantly higher yield of the methyl ether product on photolysis in 1:1 MeOH/H₂O compared with **16**, with a quantum yield ($\Phi_{\text{p}} = 0.40$) only fractionally lower than that measured for the corresponding ortho isomer **4**. More important is the fact that the transient is quenchable both electrophilically and nucleophilically since its lifetime decreased in both acidic and basic media. The deprotonated hydroxy group (σ^-) is electron-donating on the benzene ring at a meta position ($\sigma_{\text{m}} = -0.47$) unlike the hydroxy group itself, which is electron-withdrawing at the meta position ($\sigma_{\text{m}} = +0.12$). If the transients from **5** were simply the cation **31**, its expected lifetime in aqueous solution, using data from McClelland et al. (12*b*), would be less than 1 ns and hence not observable using our LFP system. Its much longer observed lifetime (30 ns) is consistent with the hydroxyl group having been deprotonated. We thus assign this transient as *m*-QM **20**. Therefore, the present method offers a simple and efficient way for photogeneration of *m*-QMs in their zwitterionic form.

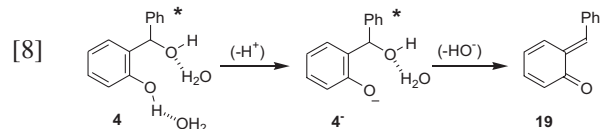
Mechanisms of reaction

There are four aspects of the reaction mechanism that can be addressed for the QMs studied in this work: (i) their photochemical mechanism(s) of formation, (ii) their thermal mechanism(s) for subsequent hydration, methanolysis, or nucleophilic attack, depending on the solvent system and nucleophiles used, (iii) [4+2] cycloaddition with added dienophiles such as ethyl vinyl ether, and (iv) self-condensation (polymerization). Thermal hydration and nucleophilic attack of photochemically generated QMs (*o* and *p*) have been studied by several other groups (5*e*–5*k*). Some initial studies of [4+2] cycloaddition have been reported (5*c*, 5*d*), but more studies are required in this area before a more complete picture is available. Therefore, only the first and last aspects will be addressed in this section.

Formation of *o*-QMs **19** and **30** from **4** and **8**, respectively, in neat CH₃CN probably involves a unimolecular dehydration pathway as shown in eq. [7]. This mechanism takes advantage of the enhanced acidity of phenols in S₁ and the presence of the nearby benzylic alcohol (hydrogen bonded as shown), which in this mechanism formally acts as hydroxide ion. When these moieties are too far from each other, the mechanism does not operate. Indeed, none of the *m* and *p* isomers give QMs on photolysis in neat CH₃CN (they all require the presence of water). The addition of small amounts of water to CH₃CN (up to 2 mol/L) resulted in reduction of yield of *o*-QM and an enhancement of fluorescence yield and lifetime. Water is expected to hydrogen bond to the phenol and alcohol OH groups and break up the internal hydrogen bond already in place. This retards the simple dehydration mechanism and hence results in a drop in yield. Addition of more water opens up a new pathway for *o*-QM formation, viz., the water-assisted mechanism shown in eq. [8]. In this mechanism, the details of the water–hydrogen bonding is not known and only one water

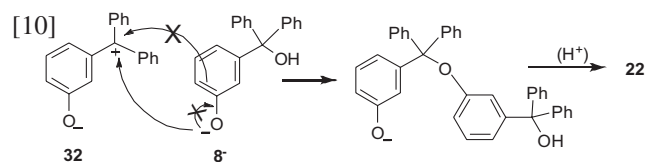
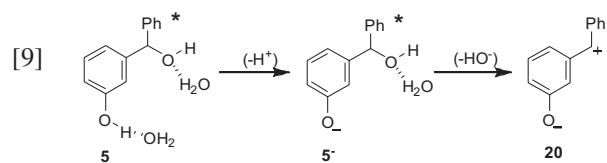


molecule is shown for hydrogen bonding to each of the substrate OH groups. Interestingly, Freccero and co-workers (5*k*) have carried out DFT calculations on the alkylation of the parent unsubstituted *o*-QM with water (in the gas phase) and found that the presence of two water molecules (one acting as a catalyst) accelerates the addition.



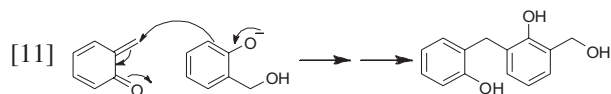
The observation that direct photolysis of the phenoate form of **4** (that is, **4⁻**) resulted in a higher quantum yield of **19** supports the notion that the reaction probably involves two steps: the ionization step ($-H^+$) and the dehydroxylation step ($-HO^-$), although a concerted mechanism cannot be ruled out. Another pathway in which loss of hydroxide ion takes place first (photodehydroxylation) to give a cation followed by deprotonation of the phenol to give the *o*-QM can be ruled out, since this would not explain the enhanced quantum yield for the formation of QMs derived from these hydroxybenzyl alcohols (**4–6**) compared with the corresponding methoxy-substituted analogs **15–17**. Indeed, for **15–17** and related compounds, a simple photodehydroxylation pathway is operative for the formation of the corresponding benzylic cations (**15**).

A similar mechanism for the formation of *m*-QM **20** that requires the presence of water is shown in eq. [9]. The difference here is that the excited state of **5⁻** is expected to have a substantial portion of the negative charge localized at the *m* position (Zimmerman ortho–meta effect (9)), hence allowing the subsequent dehydroxylation step. Deactivation back to the ground state gives rise to a zwitterionic *m*-QM **20**, which has a non-Kekulé structure. Although no polymeric material was isolated from photolysis of **5** in base, photolysis of **8** gave substantial amounts of oligomers (Scheme 1). This is because the corresponding zwitterionic *m*-QM **32** is about 1000-fold longer-lived (30 ns for **20** compared with 10 μ s for **32**). Thus, bimolecular attack by **8⁻** (eq. [10]) competes with attack by water and hydroxide ion. It is interesting to comment that *m*-QM condensation is due to attack of oxygen on the benzylic carbon, giving rise to oligomers held together with benzylic ether bonds. For comparison, the photocondensation of *o*-hydroxybenzyl alcohol (eq. [11]) results in attack via the benzene ring carbon (enolate-like attack), giving rise to phenol-formaldehyde condensation polymers (**8**). The key difference may be the increased steric



bulk of the two benzylic phenyl groups of **32**, which would hinder attack via the *o* position on the benzene ring.

In summary, QMs are the key intermediates in the



photochemistry of hydroxyl-substituted benzyl alcohols. These compounds are suitably designed to take advantage of the enhanced acidity of the phenol in S_1 and the propensity of benzylic alcohol to depart as hydroxide ion or water and its reluctance to leave as hydroxyl radical. This is unlike the situation if other leaving groups such as halides and acetate are used. Thus, hydroxyl-substituted benzyl alcohols react almost exclusively via polar or ionic intermediates. An added bonus is that they are generally fluorescent making them ideal for fluorescence studies. Other added features and uses await further discovery.

Experimental section

General

1H NMR spectra were recorded on either a PerkinElmer R32 (90 MHz), a Bruker AC 300 (300 MHz), or a Bruker AM 360 (360 MHz) instrument using $CHCl_3-d$, CH_3CN-d_3 or acetone- d_6 as solvents. Mass spectra were taken on either a Finnigan 3300 (CI) or a Kratos Concept H (EI and FAB) instruments. Melting points were determined on a Kofler hot stage microscope (uncorrected). UV–vis spectra were recorded either on a Phillips PU 8740, Varian Cary 5, or Pye Unicam SP8–400 spectrophotometer. Analytical thin layer chromatography (TLC) was performed on precoated silica gel plates (Macherey-Nagel, Sil/UV–vis₂₅₄), using solvent systems as indicated in each experiment. Preparative TLC was carried out on 20 cm \times 20 cm silica gel GF 1000 micrometer Uniplates (Analtech).

Common laboratory reagents

Methylene Chloride (A.C.S., reagent grade) was distilled before use. Anhydrous THF was obtained by distillation over potassium. Acetonitrile was either HPLC grade for photolysis, UV and LFP studies or freshly distilled over CaH_2 under N_2 for steady state fluorescence measurements. HPLC grade MeOH was stirred with $NaHCO_3$ for at least one hour to remove any trace of acid prior to photolysis. Cyclohexane (HPLC) were used as received. Deuterated solvents, including D_2O , $CDCl_3$, $(CD_3)_2CO$, and CD_3CN were purchased from Cambridge Isotopes (99.9% D). Standard buffers were purchased from Fisher. Aqueous solutions of the appropriate pH were used directly or diluted from standardized stock of NaOH or H_2SO_4 with known concentration. Prior to photolysis, pH values of the water portion were checked by a pH meter. *o*-Benzylphenol (**18**) was purchased from Sigma-Aldrich Reagents and used as received. 1H NMR and GC analysis showed that it was >98% pure. Ethanolamine (Sigma-Aldrich) was distilled before use. *o*-Methoxybenzhydrol (**15**) was available in the laboratory. 1H NMR (300 MHz, acetone- d_6) δ : 3.8 (s, 3H), 4.6 (d, 1H, D_2O

exchangeable), 6.1 (d, 1H), 6.8–7.6 (m, 9H). MS (CI) m/z : 197 ($M^+ - 17$, base peak), 215 ($M^+ + 1$). (EI) 214 (M^+).

Materials

All readily available organic and inorganic reagents required in the synthesis reported below were purchased from Sigma-Aldrich and used as received.

Grignard reaction

Magnesium was washed with dilute HCl to remove magnesium oxide and thoroughly dried. Pre-dried PhBr was dissolved in freshly distilled THF and added dropwise (under N_2) to magnesium/THF (a pinch of I_2 added) in an ice bath, which was then vigorously stirred. After the addition, the reaction mixture was refluxed for 1 h and cooled to room temperature (RT). The reacting PhMgBr was transferred to a dropping funnel and added dropwise to a THF solution of the appropriate carbonyl compound. After addition, the solution was refluxed and reaction progress monitored by NMR. Work-up consisted of the addition of saturated aq. NH_4OAc to a cooled solution to quench excess PhMgBr. Diluted HCl was also used to further acidify the solution, if required. The solution was then extracted with CH_2Cl_2 .

$NaBH_4$ reduction

The ketone was dissolved in 50–100 mL of MeOH and cooled in an ice bath. To this stirred solution, a suspension of $NaBH_4$ in ice water was added dropwise. The solution was then heated to 40–50 °C for 1–2 h. After cooling by ice, the solution was neutralized with aq. NH_4Cl and extracted with 3×50 mL of CH_2Cl_2 . The organic solvent was removed using a rotary evaporator and residue was dried on a vacuum pump.

o-Hydroxybenzhydrol (4)

Method A

To a stirred solution of salicylaldehyde (Sigma-Aldrich, 2.0 g, 17.9 mmole) in 50 mL of dry THF, 30 mL of 1.8 mol/L phenyllithium solution (54 mmole) was added under nitrogen in a dry ice–acetone bath. After reflux (4 h), the reaction mixture was cooled to RT and 50 mL of wet THF was added carefully followed by a further 10 min reflux to decompose the excess phenyllithium. The reaction mixture was then transferred to a 500 mL erlenmeyer flask, and 100 mL of ice water was added and the solution acidified with saturated NH_4Cl . The solution was extracted with diethyl ether (3×70 mL). Removal of the ether afforded an oil (3.2 g, 90%), which solidified overnight.

Method B

Following the general procedure described above for making PhMgBr, 10 g salicylaldehyde (0.08 mol) was reacted with PhMgBr (0.24 mol). The crude yellow solid was recrystallized from 1:1 toluene/hexane to afford pure **112** as white crystals, mp 86 to 87 °C. 1H NMR (300 MHz, acetone- d_6) δ : 4.3 (b, 1H, D_2O exchangeable), 6.1 (s, 1H), 6.7–7.3 (m, 9H), 8.6 (b, 1H, D_2O exchangeable). MS (CI) m/z : 183 (base peak, ($M^+ - 17$)).

3-Phenylisocoumaranone (7)

The compound was made according to the procedure of Padwa et al. (7). To an ice-cooled mixture of finely pulverized phenol (26.5 g) and mandelic acid (30.45 g) was added 80 mL of a 70% sulfuric acid solution. The mixture was stirred at 0 °C until dissolution was nearly obtained and then heated at 115 °C for 45 min. The mixture was cooled to RT, poured into 400 mL of ice water slurry, and extracted with three 100 mL portions of methylene chloride. The combined organic layers were washed with 100 mL of a saturated aqueous sodium bicarbonate solution and dried over magnesium sulfate. The evaporation of the solvent under reduced pressure gave a red liquid as the crude product. When placed under vacuum, crystals slowly formed. White crystals were obtained after recrystallization from 95% ethanol, mp 111–114 °C (lit. value (7) 113 to 114 °C). 1H NMR (300 MHz, acetone- d_6) δ : 5.2 (s, 1H), 7.1–7.5 (m, 9H). MS (CI) m/z : 211 ($M^+ + 1$, base peak), 183 ($M^+ - 28$).

m-Hydroxybenzhydrol (5)

Method A

Crude **5** was obtained by reducing *m*-hydroxybenzophenone (2.6 g, 0.013 mol) with $NaBH_4$ (0.75 g, 0.019 mol) following the general procedure.

Method B

Following the general procedure using PhMgBr, 4.3 g Mg (0.18 mol), and 27.4 g PhBr (0.18 mol) were used to make the Grignard reagent, which was reacted with 7 g of *m*-hydroxybenzaldehyde (0.057 mol) to give a brownish solid. The crude product was recrystallized from 8:1 toluene/ligroin to afford white fine needlelike crystals, mp 115 °C. 1H NMR (300 MHz, acetone- d_6) δ : 4.7 (d, 1H, D_2O exchangeable), 5.7 (d, 1H), 6.4–7.5 (m, 9H), 8.2 (s, 1H, D_2O exchangeable). MS (CI) m/z : 183 ($M^+ - 17$, base peak), 201 ($M^+ + 1$).

m-Methoxybenzhydrol (16)

Using the general procedure for PhMgBr, 10 g of *m*-anisaldehyde (0.074 mol) was reacted with PhMgBr (0.24 mol). The crude product (yellow oil) was distilled under reduce pressure to afford pure **16** (clear oil). 1H NMR (300 MHz, acetone- d_6) δ : 3.7 (s, 3H), 4.8 (d, 1H, D_2O exchangeable), 5.8 (d, 1H), 6.7–7.5 (m, 9H). MS (CI) m/z : 197 ($M^+ - 17$, base peak), 215 ($M^+ + 1$).

p-Hydroxybenzhydrol (6)

Following the general procedure for $NaBH_4$ reduction, *p*-hydroxybenzophenone (1.98 g, 0.01 mol) was reduced by $NaBH_4$ (0.75 g, 0.02 mol). The crude product was recrystallized from toluene to afford **6**, mp 159–162 °C. 1H NMR (300 MHz, acetone- d_6) δ : 4.6 (d, 1H, D_2O exchangeable), 5.7 (d, 1H), 6.4–7.5 (m, 9H), 8.2 (s, 1H, D_2O exchangeable). MS (CI) m/z : 183 ($M^+ - 17$, base peak), 201 ($M^+ + 1$).

3-Methoxy-4-hydroxybenzhydrol (10)

Following the general procedure for PhMgBr, 1 g of Mg (0.042 mol) and 6.54 g (0.042 mol) of PhBr were used to produce PhMgBr, which was subsequently reacted with

1.27 g (0.008 mol) of 3-methoxy-4-hydroxybenzaldehyde. On work-up, the resulting yellow oil was twice eluted through a silica gel column (CH_2Cl_2), which afforded **10** as a pure clear oil. ^1H NMR (300 MHz, acetone- d_6) δ : 3.4 (s, 3H), 4.6 (d, 1H, D_2O exchangeable), 5.7 (d, 1H), 5.9 (d, 1H, D_2O exchangeable), 7.0–7.5 (m, 8H). MS (CI) m/z : 213 ($\text{M}^+ - 17$), 231 (M^+).

3,5-Dibutyl-4-hydroxybenzhydrol (11)

Following the general procedure for PhMgBr , 1 g of Mg (0.042 mol) and 6.54 g (0.042 mol) of PhBr were used to produce PhMgBr , which was subsequently reacted with 3.36 g (0.014 mol) of 3,5-di-*t*-butyl-4-hydroxybenzaldehyde. The crude product was obtained as an orange solid which was recrystallized in ligroin to give white crystals, mp 123 to 124 °C. ^1H NMR (300 MHz, acetone- d_6) δ : 1.4 (s, 18H), 4.6 (d, 1H, D_2O exchangeable), 5.7 (d, 1H), 5.9 (d, 1H, D_2O exchangeable), 7.0–7.5 (m, 7H). MS (CI) m/z : 295 ($\text{M}^+ - 17$, base peak), 313 ($\text{M}^+ + 1$).

p-Methoxybenzhydrol (17)

p-Methoxybenzophenone (2 g, 0.01 mol) was reduced using NaBH_4 (4.29 g, 0.13 mol) according to the general procedure. The crude product was recrystallized from petroleum ether to give a white crystalline solid, mp 59–62 °C. ^1H NMR (300 MHz, acetone- d_6) δ : 3.7 (s, 1H), 4.7 (d, 1H, D_2O exchangeable), 5.8 (d, 1H), 6.7–7.5 (m, 9H), 8.2 (s, 1H, D_2O exchangeable). MS (CI) m/z : 197 ($\text{M}^+ - 17$, base peak), 215 ($\text{M}^+ + 1$). (EI) 214 (M^+).

α,α -Diphenyl-*o*-hydroxybenzyl alcohol (8)

Following the general procedure for PhMgBr , Mg (4.2 g, 0.17 mol) and PhBr (27 g, 0.17 mol) were used to make the PhMgBr , which then reacted with *o*-hydroxybenzoic acid methyl ester (4.5 g, 0.03 mol). The crude product was recrystallized from toluene to afford a white crystalline solid, mp 148–150 °C. ^1H NMR (360 MHz, acetone- d_6) δ : 6.4 (s/b, 1H, D_2O exchangeable), 6.4–7.5 (m, 14H), 9.1 (s/b, 1H, D_2O exchangeable); (300 MHz, CDCl_3) δ : 3.7 (s, 1H, D_2O exchangeable), 6.4–7.4 (m, 14H), 8.1 (s, 1H, D_2O exchangeable). MS (CI) m/z : 259 ($\text{M}^+ - 17$, base peak).

α,α -Diphenyl-*m*-hydroxybenzyl alcohol (9)

The methyl ester of *m*-hydroxybenzoic acid was prepared by refluxing 20 g of *m*-hydroxybenzoic acid in 400 mL of MeOH with 1 mL of concd. H_2SO_4 for 10 h. After cooling to RT, 2–4 g of NaHCO_3 was added with stirring and most of the MeOH evaporated. To this was added 200 mL of CH_2Cl_2 and the solution backwashed with water and saturated aq. NaHCO_3 . Crude *m*-hydroxybenzoic methyl ester was obtained after removal of the solvent and used without further purification.

Using the Grignard reaction procedure, 2 g of *m*-hydroxybenzoic methyl ester (0.013 mol) was reacted with PhMgBr produced from 2 g of Mg (0.083 mol) and 13 g of PhBr (0.084 mol) to generate a yellow gel as the crude product. The product was recrystallized from CH_3CN to give white crystals, mp 151 to 152 °C. ^1H NMR (300 MHz, acetone- d_6) δ : 5.2 (s, 1H, D_2O exchangeable), 6.6–7.4 (m, 14H), 8.2 (s, 1H, D_2O exchangeable). MS (CI) m/z : 199 ($\text{M}^+ - 77$, base peak), 277 ($\text{M}^+ + 1$).

m-Benzylphenol (24)

A THF solution of 2.0 g of **5** was shaken under H_2 (2 atm, 1 atm = 101.325 kPa) for 30 h. The product mixture was eluted by CH_2Cl_2 in a silica column, which gave the initial crude product. Colorless **24** was obtained by distillation under reduced pressure. ^1H NMR (300 MHz, acetone- d_6) δ : 3.9 (d, 2H), 6.6–6.8 (m, 3H), 7.0–7.4 (m, 6H), 8.2 (s, 1H, D_2O exchangeable). MS (CI) m/z : 185 ($\text{M}^+ + 1$).

General photolysis procedure

All preparative photolysis were carried out in a Rayonet RPR 100 photochemical reactor equipped with 254 lamps, using quartz tubes (100–200 mL), which were cooled with an internal cold finger (tap water, <15 °C). Solutions were continuously purged with a stream of argon via a stainless steel syringe needle for 10 min before and during the irradiation to effect stirring and deoxygenation. The length of photolysis varied from 3–60 min depending on the conversion desired. After photolysis, work-up involved adding a saturated aqueous solution of NaCl and extracting with 5 \times 75 mL portions of CH_2Cl_2 . The organic extracts were then combined and dried over MgSO_4 . Filtration of the MgSO_4 and evaporation of CH_2Cl_2 under reduced pressure provided crude photochemical products, which were then separated by preparative TLC, if necessary, and characterized by ^1H NMR and mass spectroscopy. Control experiments were repeated in the absence of light at RT (~22 °C). Possible thermal reactions in photomethanolysis were eliminated by the addition of a pinch of NaHCO_3 .

Photolysis *o*-hydroxybenzhydrol (4)

A solution of 40 mg **4** in 100 mL 1:1 $\text{H}_2\text{O}/\text{MeOH}$ (NaHCO_3 treated) was photolyzed at 254 nm. ^1H NMR analysis showed that ether **12** was the only product in low conversion runs and *o*-benzylphenol **18** was formed only in high conversion runs. Preparative TLC separation afforded pure **12**. ^1H NMR (300 MHz, acetone- d_6) δ : 3.3 (s, 3H), 5.7 (s, 1H), 6.7–7.4 (m, 9H), 8.5 (s, 1H, D_2O exchangeable). MS (CI) m/z : 183 ($\text{M}^+ - 31$, base peak). The identity of **18** was confirmed by comparison with an authentic sample.

Photolysis *p*-hydroxybenzhydrol (6)

A solution of 40 mg of **6** in 100 mL 1:1 $\text{H}_2\text{O}/\text{MeOH}$ (NaHCO_3 treated) was photolyzed at 254 nm for 3 min. Methyl ether **14** was the only product purified by preparative TLC. ^1H NMR (300 MHz, acetone- d_6) δ : 2.9 (s, 3H), 5.2 (s, 1H), 6.6–7.4 (m, 9H), 8.3 (b, 1H, D_2O exchangeable). MS (CI) m/z : 121 ($\text{M}^+ - 93$, base peak), 183 ($\text{M}^+ - 31$), 215 ($\text{M}^+ + 1$).

Photolysis of 3-phenylisocoumaranone (7)

A solution of 40 mg of **7** in 100 mL 1:1 $\text{H}_2\text{O}/\text{MeOH}$ was photolyzed at 254 nm for 3 min. The ^1H NMR of the product mixture showed that ~3% of **12** was formed, as indicated by the characteristic methoxy singlet at δ 3.3 (s, 3H) and methine singlet at δ 5.7 (s, 1H).

Photolysis of α,α -diphenyl-*o*-hydroxybenzyl alcohol (8)

A solution of 55 mg of **8** in 100 mL 1:1 $\text{H}_2\text{O}/\text{MeOH}$ (NaHCO_3 treated) was photolyzed at 254 nm for 3 min. The product was its corresponding methyl ether (28%), purified

by preparative TLC. ^1H NMR (300 MHz, acetone- d_6) δ : 3.2 (s, 3H), 5.6 (s, 1H), 6.4–7.8 (m, 14H), 8.7 (s, 1H, D_2O exchangeable). MS (CI) m/z : 259 ($\text{M}^+ - 31$, base peak).

Photolysis *m*-hydroxybenzhydrol (5)

A solution of 100 mg of **5** was dissolved in 100 mL 1:1 $\text{H}_2\text{O}/\text{MeOH}$ and photolyzed at 254 nm for 5, 30, and 60 min, respectively. The product mixture contained **13** (methoxy singlet δ 3.3 (s, 3H)) and **24** (methylene δ 3.9 (d, 2H) both of which were purified by preparative TLC. Compound **13**: ^1H NMR (300 MHz, acetone- d_6) δ : 3.2 (s, 3H), 5.2 (s, 1H), 6.3 (s, 1H), 6.8–7.8 (m, 18H), 8.3 (s, 1H, D_2O exchangeable); MS (FAB/LSIMS, *m*-NBA as Matrix) m/z : 395 ($\text{M}^+ - 1$, base peak). Product **24**: ^1H NMR (300 MHz, acetone- d_6) δ : 3.9 (s, 2H), 6.6–6.8 (m, 3H), 7.0–7.4 (m, 6H), 8.3 (s, 1H, D_2O exchangeable).

Photolysis of α -phenyl-*m*-hydroxybenzhydrol (9)

A solution of 55 mg of **9** in 100 mL 1:1 $\text{H}_2\text{O}/\text{MeOH}$ (NaHCO_3 treated) was photolyzed at 254 nm for 3 min. The product was the corresponding methyl ether (10%), which was purified by preparative TLC. ^1H NMR (300 MHz, acetone- d_6) δ : 3.0 (s, 3H), 6.6–7.4 (m, 14H), 8.2 (s, 1H, D_2O exchangeable). MS (CI) m/z : 259 ($\text{M}^+ - 31$, base peak), 291 ($\text{M}^+ + 1$).

A solution of 200 mg of **9** was dissolved in 200 mL of neat water (pH 12) and photolyzed at 254 for 30 min (vigorous Ar purge), which resulted in very cloudy (milky) solution. The product mixture was worked up by adding large amounts of aq. NH_4Cl to aggregate the fine pale yellowish precipitate, which was then filtered out of the solution and allow to dry on the filter paper. ^1H NMR (300 MHz, acetone- d_6) showed that a new product was formed (>80%) which was identified as condensation product **22**, δ : 5.1 (s, 1H, D_2O exchangeable), 6.4 (t, 1H), 6.6–7.4 (m, 27H), 8.2 (s, 1H, D_2O exchangeable). Negative FAB/LSIMS (*m*-NBA as matrix) m/z : 533 ($\text{M}^+ - 1$, base peak).

A solution of 100 mg of **9** in 100 mL 1:1:2 1 mol/L of NaOH solution/ $\text{H}_2\text{O}/\text{CH}_3\text{CN}$ was photolyzed at 254 nm for 30 min. A clear and pale yellow solution was obtained. To this solution, 300 mL of water was added to give milky solution, which aggregated upon the addition of aq. NH_4Cl . The yellow precipitate thus obtained was filtered out and allowed to dry on filter paper. Negative FAB/LSIMS (*m*-NBA as Matrix) 258 ($\text{M}^+ - 18$, base peak), $n \times 258 + 275$ (n from 1 to 10, see Fig. 2). Therefore, the product was identified as a mixture of oligomers **23**.

Steady-state fluorescence and lifetime measurements

Steady-state fluorescence spectra (uncorrected) were recorded on a PerkinElmer MPF-66 or Photon Technology International (PTI) A-1010 fluorimeter. Fluorescence lifetimes were obtained by a PTI LS-1 time-correlated single photon counting system using a hydrogen flash lamp as the excitation source ($\lambda_{\text{ex}} = 270$ nm), with data fit using the iterative deconvolution program. Each sample ($\sim 10^{-5}$ mol/L, OD < 0.02) was prepared in 3.0 mL four-sided suprasil quartz cuvettes with flat transparent bottoms and saturated with a stream of Ar (10 min) prior to the measurement. Absolute fluorescence quantum yields (Φ_f) were measured in CH_3CN , using anisole ($\Phi_f = 0.29$ in cyclohexane) (10) as external

standard. Excitation wavelength was 275 nm. OD₂₇₅ was measured for individual sample and kept at ~ 0.1 .

Laser Flash Photolysis (LFP)

Nanosecond laser flash photolysis (LFP) experiments were carried out at the University of Victoria LFP Facility at 20 ± 2 °C. A Spectra Physics YAG laser Model GCR-12 (266 nm, ≤ 70 mJ/pulse) was used as excitation source. The laser pulse energies were typically attenuated to less than 20mJ/pulse by adjusting the high voltage for the flash lamp to avoid multiple photon process. The analyzing beam employed consists of a pulsed 150 W xenon lamp (Oriel housing Model 66057, PTI power supply Model LPS-220). Generally, a solution of OD₂₆₆ ≤ 0.3 was prepared by dilution from a stock solution, followed by 10 min prepurge of oxygen or nitrogen. Experiments were carried out in a flow system (7 mm \times 7 mm quartz cell) with continuous purge of oxygen or nitrogen.

Acknowledgments

This research was supported by the Natural Sciences and Engineering Research Council (NSERC) of Canada and the University of Victoria. We thank Cheng Yang for initial contributions in this study.

References

- (a) P. Wan, S. Culshaw, and K. Yates. *J. Am. Chem. Soc.* **104**, 2509 (1982); (b) P. Wan and K. Yates. *Rev. Chem. Intermed.* **5**, 157 (1984).
- (a) J.F. Ireland and P.A.H. Wyatt. *Adv. Phys. Org. Chem.* **12**, 131 (1976); (b) P. Wan and D. Shukla. *Chem. Rev.* **93**, 571 (1993).
- K. Yates and P. Kalandropoulos. *J. Am. Chem. Soc.* **108**, 6290 (1986).
- R.W. Van De Water and T.R.R. Pettus. *Tetrahedron*, **58**, 5367 (2002).
- Representative papers: (a) P. Seiler and J. Wirz. *Helv. Chim. Acta*, **55**, 2693 (1972); (b) T.W. Lewis, D.Y. Curtin, and I.C. Paul. *J. Am. Chem. Soc.* **101**, 5717 (1979); (c) L. Diao, C. Yang, and P. Wan. *J. Am. Chem. Soc.* **117**, 5369 (1995); (d) P. Wan, B. Barker, L. Diao, M. Fischer, Y. Shi, and C. Yang. *Can. J. Chem.* **74**, 465 (1996); (e) K. Nakatani, N. Higashida, and I. Saito. *Tetrahedron Lett.* **38**, 5005 (1997); (f) Y. Chiang, A.J. Kresge, and Y. Zhu. *J. Am. Chem. Soc.* **122**, 9854 (2000); (g) Y. Chiang, A.J. Kresge, and Y. Zhu. *Pure Appl. Chem.* **72**, 2299 (2000); (h) Y. Chiang and A.J. Kresge. *Org. Biomol. Chem.* **2**, 1090 (2004); (i) R.A. McClelland, M.M. Moriarty, and J.M. Chevalier. *J. Chem. Soc. Perkin Trans. 2*, 2235 (2001); (j) E. Modica, R. Zanaletti, M. Freccero, and M. Mella. *J. Org. Chem.* **66**, 41 (2001); (k) C.D. Valentin, M. Freccero, R. Zanaletti, and M. Sarzi-Amade. *J. Am. Chem. Soc.* **123**, 8366 (2001); (l) S.N. Richter, S. Maggi, S. Colloredo-Mels, M. Palumbo, and M. Freccero. *J. Am. Chem. Soc.* **126**, 13973 (2004); (m) E.E. Weinert, R. Dondi, S. Colloredo-Mels, K.N. Frankenfield, C.H. Mitchell, M. Freccero, and S. Rokita. *J. Am. Chem. Soc.* **128**, 11940 (2006); (n) S. Colloredo-Mels, F. Doria, D. Verga, and M. Freccero. *J. Org. Chem.* **71**, 3889 (2006).
- (a) P. Wan and E. Krogh. *J. Am. Chem. Soc.* **111**, 4887 (1989); (b) A. Blazek, M. Pungente, E. Krogh, and P. Wan. *J.*

- Photochem. Photobiol. A, **64**, 315 (1992); (c) C. Yang and P. Wan. J. Photochem. Photobiol. A, **80**, 227 (1994).
7. A. Padwa, D. Dehm, T. Oine, and G. Lee. J. Am. Chem. Soc. **97**, 1837 (1975).
 8. P. Wan and D. Hennig. J. Chem. Soc. Chem. Commun. 939 (1987).
 9. (a) H.E. Zimmerman. J. Am. Chem. Soc. **117**, 8988 (1995); (b) H.E. Zimmerman. J. Phys. Chem. A, **102**, 5616 (1998).
 10. I.B. Berlman. Handbook of fluorescence spectra of aromatic molecules. 2nd ed. Academic Press, NY. 1971.
 11. J. Chateaufneuf. J. Chem. Soc. Chem. Commun. 1437 (1991).
 12. (a) J. Bartl, S. Steenken, H. Mayr, and R.A. McClelland. J. Am. Chem. Soc. **112**, 6918 (1990); (b) R.A. McClelland, V.M. Kanagasabapathy, N.S. Banait, and S. Steenken. J. Am. Chem. Soc. **111**, 3966 (1989).
 13. K.S. Peters and B. Li. J. Phys. Chem. **98**, 401 (1994).
 14. S. Hamai and H. Kokubun. Bull. Chem. Soc. Jpn. **47**, 2085 (1974).
 15. P. Wan and B. Chak. J. Chem. Soc. Perkin Trans. 2, 1751 (1986).